Clinical and Angiographic Characteristics of Patients Likely to Have Vulnerable Plaques

Analysis From the PROSPECT Study

Christos V. Bourantas, MD, PHD,* Hector M. Garcia-Garcia, MD, PHD,*
Vasim Farooq, MBCHB,* Akiko Maehara, MD,† Ke Xu, PHD,† Philippe Généreux, MD,†
Roberto Diletti, MD,* Takashi Muramatsu, MD, PHD,* Martin Fahy, MSC,†
Giora Weisz, MD,† Gregg W. Stone, MD,† Patrick W. Serruys, MD, PHD*

Rotterdam, the Netherlands; and New York, New York

OBJECTIVES This study sought to determine the clinical and angiographic variables that would identify patients with high-risk "vulnerable" coronary plaques.

BACKGROUND In the PROSPECT (Providing Regional Observations to Study Predictors of Events in the Coronary Tree) study, in patients successfully treated for acute coronary syndrome (ACS), plaque composition, plaque burden, and minimal luminal area as detected by 3-vessel radiofrequency intravascular ultrasound (IVUS) imaging were associated with an increased risk of developing future events from untreated atherosclerotic lesions (vulnerable plaques). Whether baseline demographic and angiographic findings can be used to identify patients most likely to have vulnerable coronary plaques has not been examined.

METHODS On the basis of 3-vessel radiofrequency IVUS imaging, patents in the PROSPECT trial were classified in 2 groups according to whether or not one or more untreated high-risk plaques were present, defined as having ≥ 2 high-risk features (a thin-cap fibroatheroma, plaque burden $\geq 70\%$, and/or minimal luminal area ≤ 4 mm^2).

RESULTS The high-risk group (those with one or more high-risk lesions) had higher Framingham risk score (7.5 ± 3.4 vs. 6.9 ± 3.3; p = 0.04), more extensive coronary artery disease, and more nonculprit lesion–related cardiovascular events during the 3-year follow-up (hazard ratio: 2.63; 95% confidence interval: 1.62 to 3.66; p < 0.0001). However, demographic factors had poor discrimination in detecting high-risk patients (area under the curve 0.55), and discrimination was only slightly improved when angiographic variables were entered into the model (area under the curve 0.64).

CONCLUSIONS Clinical and angiographic characteristics had poor predictive accuracy in identifying patients with untreated high-risk plaques related to future adverse events. This finding highlights the potential value of comprehensive 3-vessel imaging assessment (either invasive or noninvasive) to evaluate plaque phenotype for more accurate risk stratification of patients admitted with ACS. (J Am Coll Cardiol Img 2013;6:1263–72) © 2013 by the American College of Cardiology Foundation

ntravascular ultrasound (IVUS) with radio-frequency backscatter analysis provides visualization of the entire vessel wall; assessment of the luminal, outer vessel wall, and plaque dimensions; and reliable semiautomated detection of plaque components and quantification of their burden (1,2). This imaging modality is therefore useful in the research of atherosclerosis (3,4). Several studies used serial backscatter analysis of IVUS signal examinations to assess changes in the composition of the plaque and the effect of pharmaceutical treatment (5–7). In the recently reported PROSPECT

(Providing Regional Observations to Study Predictors of Events in the Coronary Tree) study, 3-vessel IVUS–virtual histology (VH) imaging was used to evaluate the prognostic implications of the composition of the plaque and its burden in patients admitted with acute coronary syndrome (ACS) (6). Consistent with prior pathological studies, the PROSPECT trial demonstrated that plaque composition, as well as burden, were predictors of future cardiovascular events (6,8).

The 3 characteristics in the PROSPECT trial that were associated with future adverse lesion-specific cardiovascular events, namely plaque burden, minimal luminal area, and thin-cap fibroatheroma (TCFA) as defined by IVUS-VH, required 3-vessel catheter-based interrogation for identification, a procedure not without risk (6). Several studies have shown that the composition and extent of atheroma are associated with cardiovascular risk factors and that they differ in patients admitted with different clinical presentations (3,9–12). Therefore, baseline demographics or a combination of clinical and angiographic variables may allow detection of patients who have lesions with plaque features related to an increased risk for cardiovascular events, possibly allowing a targeted approach to imaging. The aim of the present analysis was therefore to identify clinical and angiographic characteristics related to the high-risk plaques in the PROSPECT study and to construct a model that will allow accurate detection of patients with a vulnerable plaque phenotype.

METHODS

Study population. The design, inclusion and exclusion criteria, and endpoints and definitions of the

ABBREVIATIONS AND ACRONYMS

ACS = acute coronary syndrome

CRP = C-reactive protein

EEM = external elastic membrane

IVUS = intravascular ultrasound

MACE = major adverse cardiac events

MLA = minimum lumen area

QCA = quantitative coronary angiography

TCFA = thin-cap fibroatheroma

VH = virtual histology

PROSPECT study have already been described in detail (6). The PROSPECT trial included 697 patients admitted for an acute coronary event (i.e., ST-segment elevation myocardial infarction, non–ST-segment elevation myocardial infarction, or unstable angina) who had successful percutaneous coronary intervention in all culprit lesions. The studied patients underwent coronary angiography and 3-vessel grayscale and IVUS-VH (Volcano Corp., San Diego, California) imaging of the proximal 6- to 8-cm coronary segments using a synthetic aperture array, 20 MHz, 3.2-Fr catheter (Eagle Eye, Volcano Corp.), after intracoronary nitroglycerin administration.

Data analysis. The acquired angiographic, IVUS, and IVUS-VH data were transferred to an independent core laboratory (Cardiovascular Research Foundation, New York, New York) and analyzed, blinded to the baseline and clinical characteristics. Quantitative coronary angiographic (QCA) analysis was performed, with the use of the software Medis CMS (version 7.0, Leiden, the Netherlands) in the entire length of the coronaries and the side branches that had a reference diameter >1.5 mm. All stenoses >30% on coronary angiography were analyzed, and the following metrics were obtained: lesion length, reference diameter, minimal lumen diameter, and diameter stenosis. Lesions related to the event were characterized as culprit and the rest as nonculprit lesions.

IVUS and IVUS-VH analysis was conducted with the use of QCU-CMS (Medis) software for contouring, pcVH 2.1 (Volcano Corp.) for contouring and data output, and proprietary software (qVH, Cardiovascular Research Foundation) for segmental qualitative and quantitative output. The external elastic membrane (EEM) and the lumen borders were detected at approximately every 0.5-mm interval (depending on the heart rate and the R-R interval) and used to determine the EEM area, lumen area, and plaque area and burden (defined as $100 \times$ plaque area/EEM area). Nonculprit IVUS lesions were defined as >3 consecutive IVUS frames visualizing segments with a plaque burden ≥40%. IVUS-VH allows characterization of 4 different plaque components that are portrayed in a color-coded map, with the red corresponding to the necrotic core, green to fibrous tissue, light green to fibrofatty, and white to dense calcium. Based on its compositional traits, each lesion was classified as TCFA, thick-cap fibroatheroma, pathological intimal thickening, fibrotic plaque, and fibrocalcific plaque (2).

The IVUS-derived independent lesion characteristics, which were associated with future adverse

cardiac events (i.e., presence of a TCFA, plaque burden $\geq$70%, and minimal lumen area $\leq$4 mm^2) were used to classify the study population into 2 groups: the high-risk group included patients who had at least 1 lesion, with $\geq$2 of the 3 high-risk characteristics, whereas the low-risk group included the remaining patients, those without any high-risk lesions (6,9).

Clinical endpoints. The primary endpoint of the PROSPECT study was the composite incidence of major adverse cardiac events (MACE), consisting of cardiac death or arrest, myocardial infarction, or rehospitalization for unstable or progressive angina, as adjudicated by an independent clinical events committee. MACE were classified as related to culprit lesions if they arose from a previously treated lesion or not related to culprit lesions if they arose from an untreated lesion. If follow-up angiography was not performed, the lesion causing the event was classified as indeterminate.

Statistical analysis. Continuous variables are presented as median with 25th and 75th percentiles or mean $\pm$ SD, and binary variables are shown as absolute values and percentages. The Mann-Whitney *U* test was used for independent 2-sample comparisons of continuous variables, and the Fisher exact test was used to compare binary variables.

Graphical plots were made by the Kaplan-Meier method. The log-rank statistic was used to compare prognosis between the 2 groups. Cox regression analysis was performed to identify independent predictors of cardiovascular events. The proportionality of hazards assumption was examined by residual plotting.

Binary logistic regression analysis was performed to identify factors associated with the high-risk group. Variables with a p value <0.2 were used to construct a multivariable model. In case of collinearity (r > 0.8 and p < 0.05), the variables that had a higher level of significance were eligible for inclusion in the multivariable model. A p value <0.05 (2 tailed) was considered statistically significant. A risk score was assigned to each independent predictor based on the odds ratio (OR), and a total risk score was then calculated for each patient. The discriminatory capability of the developed score to identify patients that belonged to the high-risk group was assessed using the area under the receiver-operating characteristics curve. Data analysis was performed using SAS version 9.2 (SAS Institute, Cary, North Carolina).

RESULTS

Patient characteristics. From the 697 patients recruited in the PROSPECT study, 609 patients were included in the current analysis because 88 patients did not have complete 3-vessel IVUS-VH examinations. The patients allocated to the high-risk group were more likely to have a higher Framingham risk score and increased triglyceride levels. No other significant differences were noted in the baseline demographics between the 2 groups (Table 1).

Angiographic findings. The results of the QCA analysis are shown in Table 2. A total of 609 lesions were identified in the high-risk (n = 200) and 897 in the low-risk (n = 409) groups. The high-risk group had more extensive coronary artery disease with a greater number of nonculprit lesions and diseased coronary arteries and side branches. There were no differences in the maximum diameter stenosis of the nonculprit lesions or the angiographic characteristics of these stenoses.

IVUS and IVUS-VH findings. IVUS identified 3,014 lesions, of which 1,097 were detected in the high-risk (n = 200) and 1,917 in the low-risk (n = 409) groups. The length of the diseased segments was greater in the high-risk patients who also had a smaller mean EEM and lumen area; there were no differences between the 2 groups in the mean plaque area (Table 3). As expected by the criteria used to create the groups, high-risk, compared with low-risk, patients had a higher incidence of lesions with a minimum lumen area (MLA) $\leq$4 mm^2 (31.8% vs. 11.4%; p < 0.0001) and plaque burden $\geq$70% (18.4% vs. 3.3%; p < 0.0001). In contrast to QCA, IVUS revealed significant differences between the 2 groups in the luminal dimensions at the site of the nonculprit lesions, with the high-risk group having a smaller MLA. IVUS-VH analysis showed that the lesions in high-risk patients had a greater proportion of necrotic core and dense calcium, whereas lesions in low-risk patients had significantly more fibrofatty tissue. Accordingly, TCFAs were more frequently present in the high-risk group, whereas pathological intimal thickening was more prevalent in the low-risk group.

Clinical outcomes. Online Table 1 demonstrates the cumulative 3-year event rate (overall, culprit related, nonculprit related, and undetermined) in the overall study population and the high-risk and low-risk groups. The high-risk group had an increased rate of nonculprit lesion MACE, driven mainly by a higher rehospitalization rate due to unstable or progressive angina symptoms. High-risk status was a predictor of nonculprit lesion–related MACE by univariable analysis (hazard ratio: 2.63; 95% confidence interval [CI]: 1.62 to 3.66; p < 0.0001)

Table 1. Baseline Characteristics of the Study Population and the High-Risk and Low-Risk Groups

	Study Population (N = 609)	High-Risk Group (n = 200)	Low-Risk Group (n = 409)	p Value
Age, yrs	58.2 (50.7–67.2)	57.7 (50.4–67.1)	58.5 (50.9–67.2)	0.74
Male	466 (77)	154 (77)	312 (76)	0.84
Height, cm	173 (166–178)	172 (168–178)	173 (165–178)	0.33
Weight, kg	83 (73–95)	83 (73–94)	82.5 (73–96)	0.99
Body mass index, kg/m^2	27.9 (25.1–31.2)	28.2 (25.3–31.0)	27.9 (25.1–31.4)	0.52
Systolic blood pressure, mm Hg	130 (118–145)	135 (119–150)	130 (117–142)	0.056
Diastolic blood pressure, mm Hg	75 (68–84)	75 (68–84)	75 (68–83)	0.88
Clinical presentation				
ST-segment elevation MI	179 (29)	62 (31)	117 (29)	0.54
Non–ST-segment elevation MI	407 (67)	131 (66)	276 (68)	0.63
Unstable angina	23 (4)	7 (4)	16 (4)	0.80
History of CAD	80 (13)	30 (16)	50 (12)	0.27
History of coronary intervention	65 (11)	22 (11)	43 (11)	0.84
Congestive heart failure	12 (2)	3 (2)	9 (2)	0.76
Family history of CAD	244 (46)	82 (49)	162 (44)	0.23
Hypertension	285 (47)	102 (52)	183 (45)	0.12
Hypercholesterolemia	252 (45)	88 (47)	164 (44)	0.56
Diabetes mellitus	107 (17)	43 (22)	64 (16)	0.07
Metabolic syndrome	286 (49)	104 (53)	182 (46)	0.12
Framingham risk score	7 (5–9) 7.1 ± 3.3	7 (5–9) 7.5 ± 3.4	7 (5–9) 6.9 ± 3.3	0.04
History of tobacco use	287 (48)	98 (50)	189 (47)	0.57
eGFR, ml/min/1.73 m^2*	98 (76.2–123.4)	98.4 (78–121.1)	97.8 (75.3–124.7)	0.91
Total cholesterol, mg/dl	172 (149–202)	173 (150–202)	172 (149–202)	0.53
HDL-cholesterol, mg/dl	38.6 (34.0–47.0)	38.6 (33.0–48.0)	38.6 (34.0–45.0)	0.72
LDL-cholesterol, mg/dl	101.7 (80.4–129.0)	102.0 (81.2–129–8)	101 (79.2–128.2)	0.88
Triglycerides, mg/dl	125.0 (86.6–177.1)	138 (95.0–177.1)	121.5 (88.6–177.1)	0.04
Baseline C-reactive protein, mg/dl	7.0 (2.4–18.7)	6.8 (2.5–19.5)	7.0 (2.3–18.4)	0.88
Medications at discharge				
Statins	521 (86)	177 (89)	344 (85)	0.19
Aspirin	591 (97)	193 (97)	398 (97)	0.58
Clopidogrel/ticlopidine	591 (97)	196 (98)	395 (97)	0.33
RAAS inhibitors	411 (67)	142 (71)	269 (66)	0.21
Beta-blockers	552 (91)	185 (93)	367 (90)	0.27
Diabetic medications (insulin or other)	94 (16)	39 (20)	55 (14)	0.052

Values are median (25th and 75th percentiles), n (%), or mean ± SD. *eGFR was computed using the Modification of Diet in Renal Disease formula (38).
CAD = coronary artery disease; eGFR = estimated glomerular filtration rate; HDL = high-density lipoprotein; LDL = low-density lipoprotein; MI = myocardial infarction; RAAS = renin-angiotensin-aldosterone system.

(Fig. 1) and by multivariable Cox regression analysis (hazard ratio: 2.45; 95% CI: 1.48 to 4.04; p = 0.006).

Factors associated with the high-risk group. Variables from Tables 1 and 2 with p < 0.2 associated with the presence of at least 2 of the 3 high-risk plaque characteristics are shown in Table 4. Multivariable analysis, performed including only the clinical variables, showed that only the Framingham score was independently associated with the presence of high-risk plaque characteristics (OR: 1.05; 95% CI: 1.00 to 1.11; p = 0.047), although with poor discrimination in detecting patients belonging to the high-risk group (optimal cutoff value for the Framingham risk score 8; area under the curve 0.55). When the angiographic findings were

Table 2. Quantitative Coronary Angiographic Findings in the Study Population and the High-Risk and Low-Risk Groups

	Study Population (N = 609)	High-Risk Group (n = 200)	Low-Risk Group (n = 409)	p Value
Number of vessels with culprit lesions	1 (1–2) 1.29 ± 0.46	1 (1–2) 1.35 ± 0.48	1 (1–2) 1.27 ± 0.44	0.035
Number of epicardial vessels with nonculprit lesions	1 (1–2) 1.41 ± 0.98	2 (1–2) 1.56 ± 0.97	1 (1–2) 1.34 ± 0.98	0.007
Maximum diameter stenosis, %	46 (38–58)	47 (39–57)	45 (37–59)	0.72
Total length of nonculprit lesions, cm	20.0 (8.4–37.0)	26.3 (13.6–44.7)	16.8 (6.7–33.0)	<0.0001
Number of nonculprit lesions	2 (1–4)	3 (2–4)	2 (1–3)	<0.0001
Presence of lesions in side branches	199 (33)	87 (44)	112 (27)	<0.0001
Thrombotic lesions	0 (0–0) 0.01 ± 0.09	0 (0–0) 0.00 ± 0.00	0 (0–0) 0.01 ± 0.11	0.12
Calcified lesions	0 (0–0) 0.04 ± 0.23	0 (0–0) 0.05 ± 0.24	0 (0–0) 0.04 ± 0.23	0.51

Values are median (25th and 75th percentiles), mean ± SD, or n (%).

included in the multivariable model, only the number of nonculprit lesions (OR: 1.17; 95% CI: 1.07 to 1.29; p = 0.001) and the number of side branches affected (OR: 1.54; 95% CI: 1.04 to 2.28; p = 0.031) were independently related to the high-risk group. The combination of demographic and angiographic factors slightly improved the discrimination of the model (optimal cutoff value for the number of nonculprit lesions was 1 and for the number of side branches affected was 1; area under the curve 0.64) (Fig. 2).

DISCUSSION

The present analysis examined the association between clinical and angiographic characteristics and high-risk coronary plaque phenotype in patients treated for an acute coronary event. We found that: 1) patients with ≥2 IVUS-VH–derived plaque features related to future adverse events had a higher Framingham risk score and more extensive coronary artery disease on coronary angiography; and 2) the information provided by the patient's medical history and coronary angiography does not sufficiently discriminate among patients with versus without high-risk plaques to obviate the need for more intensive imaging.

Several prior studies have used IVUS-VH to explore the relationship between clinical factors and plaque composition (10,11,13). Philipp et al. (10) found that women were more likely to have calcified coronary arteries and a lower plaque burden and that patients with diabetes had an increased necrotic core component. Missel et al. (13) reported that lipid profile and smoking history were associated with the ratio of necrotic core to dense calcium. In

another study, Marso et al. (11) showed that patients with a high cardiovascular risk profile, estimated by the Framingham risk model, were more likely to have TCFA phenotype stenoses compared with low-risk patients. A significant limitation of all of these studies, however, is that IVUS-VH examination was restricted to the culprit vessel, and thus, the measured plaque components may not reflect the composition of the atheroma in the entire coronary tree.

The present study, as the first to use 3-vessel IVUS-VH imaging, overcomes this limitation. Also, in contrast to previous reports, we focused on identification of the patients with lesions containing ≥2 high-risk plaque features because the PROSPECT study found a relationship between the number of high-risk plaque characteristics and the subsequent nonculprit lesion–related event rate (6). Similarly to Marso et al. (9), we found an increased Framingham risk score in the high-risk group but no other significant differences in the baseline demographic characteristics between patients with and without high-risk plaques. This finding may be at least partially attributed to the fact that the PROSPECT trial enrolled a uniform patient population, all of whom had ACS. Prior studies have demonstrated differences in plaque composition in patients admitted with different clinical syndromes, with the likelihood of TCFAs being increased in those with ACS compared with stable angina (3,4). In our study, clinical variables had poor discrimination in identifying high-risk plaque characteristics.

This finding can be attributed to the multifactorial etiology of coronary atherosclerosis, which is modulated not only by clinical factors but also by

Table 3. IVUS and IVUS-VH Findings of Nonculprit Lesions in the Study Population and the High-Risk and Low-Risk Groups

	Study Population (N = 609)	High-Risk Group (n = 200)	Low-Risk Group (n = 409)	p Value
Gray-scale IVUS				
Entire lesion				
Total lesion length, mm	73.3 (45.8–103.8)	96.5 (72.5–124.8)	61.9 (38.8–90.3)	<0.0001
Average EEM CSA, mm^2	16.12 (13.91–18.62)	15.35 (13.59–17.25)	16.66 (14.21–19.16)	<0.0001
Average lumen CSA, mm^2	8.11 (6.87–9.49)	7.33 (6.33–8.62)	8.55 (7.20–9.86)	<0.0001
Average plaque area, mm^2	7.88 (6.80–9.34)	7.81 (6.90–9.19)	7.91 (6.75–9.54)	0.63
Lesion with the smallest MLA per patient				
Lesion length, mm	11.38 (5.77–21.54)	13.93 (6.60–25.75)	10.10 (5.32–18.56)	<0.0001
EEM cross-sectional area, mm^2	14.16 (10.60–18.23)	13.51 (10.06–17.45)	14.55 (10.98–18.83)	<0.0001
MLA, mm^2	5.88 (4.32–8.08)	5.14 (3.77–7.17)	6.29 (4.76–8.57)	<0.0001
Plaque area, mm^2	7.82 (5.82–10.60)	7.76 (5.85–10.59)	7.84 (5.81–10.60)	0.86
Plaque burden, %	55.4 (49.1–62.8)	58.7 (51.6–66.5)	53.7 (48.2–60.6)	<0.0001
Remodeling index	0.94 (0.85–1.00)	0.93 (0.84–1.00)	0.94 (0.85–1.00)	0.11
IVUS-VH				
Entire lesion				
Average necrotic core area, mm^2	0.50 (0.30–0.78)	0.68 (0.42–0.97)	0.45 (0.26–0.67)	<0.0001
Average fibrous tissue area, mm^2	2.54 (1.91–3.24)	2.63 (2.00–3.23)	2.52 (1.88–3.24)	0.43
Average fibrofatty tissue area, mm^2	0.84 (0.54–1.27)	0.77 (0.47–1.05)	0.90 (0.57–1.38)	0.0007
Average dense calcium area, mm^2	0.21 (0.11–0.40)	0.28 (0.16–0.46)	0.19 (0.10–0.35)	<0.0001
MLA site				
Necrotic core area, mm^2	0.48 (0.19–1.01)	0.65 (0.28–1.24)	0.39 (0.16–0.85)	<0.0001
Fibrous tissue area, mm^2	2.66 (1.65–4.13)	2.76 (1.65–4.24)	2.64 (1.66–4.03)	0.24
Fibrofatty tissue area, mm^2	0.79 (0.33–1.52)	0.67 (0.26–1.33)	0.85 (0.37–1.64)	<0.0001
Dense calcium area, mm^2	0.15 (0.03–0.44)	0.22 (0.06–0.54)	0.12 (0.02–0.37)	<0.0001
Lesion phenotype				
Thin-cap fibroatheroma	22.3	34.9	14.9	<0.0001
Thick-cap fibroatheroma	37.9	35.9	39.0	0.090
Pathological intimal thickening	36.2	26.3	42.0	<0.0001
Fibrotic	2.5	1.9	2.9	0.10
Fibrocalcific	1.1	1.0	1.2	0.67

Values are median (25th and 75th percentiles) or %.
CSA = cross-sectional area; EEM = external elastic membrane; IVUS = intravascular ultrasound; MLA = minimum lumen area; VH = virtual histology.

vessel wall inflammation, genotype, and local hemodynamic factors. In the PROSPECT trial, the baseline level of C-reactive protein (CRP), a biomarker associated with vascular inflammation, was not related to high-risk plaque characteristics. This may be due to the fact that baseline CRP level was increased by the acute coronary event, which masked the effect of chronic vascular inflammation (14–16). CRP measurements at follow-up were not considered in our analysis.

Characteristics of several other biomarkers that have been associated with future adverse cardiac events (i.e., myeloperoxidase, A2 phospholipase, blood monocyte subset counts, pregnancy-associated plasmaprotein A, and patients' hematology profiles) and are likely to affect plaque's phenotype were not available in this study (7,17–19). Currently, the European Collaborative Project on Inflammation and Vascular Wall Remodeling in Atherosclerosis–Intravascular Ultrasound trial

(NCT01789411) is underway and aims to examine the prognostic value of circulating chemokines and their association with plaque's phenotype, as determined by IVUS-VH. Genotype has been shown to affect atherosclerotic evolution, and several reports have provided evidence that vessel geometry (especially in bifurcations) affects local endothelial shear stress through which mechano-receptors influence plaque metabolism and progression (20–22).

Although the number of nonculprit lesions and the number of side branches affected was independently associated with the presence of high-risk plaques, the inclusion of QCA-derived measures had a minor impact on the predictive accuracy of the multivariable model. These findings are in agreement with a recent report that demonstrated a weak correlation between the presence of lipid-rich plaques (as detected by near-infrared spectroscopy) and the SYNTAX (Synergy Between PCI With Taxus and Cardiac Surgery) score (23). Angiography is limited to the visualization of luminal anatomy and does not provide meaningful information about the composition of plaque.

Over the last several years, numerous clinically derived risk scores have been developed to predict outcomes in patients presenting with ACS (24–28). These risk stratification models are moderately capable of predicting mortality, but they have a low discrimination in predicting future events (29). To address this limitation, several new scores have been proposed that combine clinical with biochemical or angiographic variables. However, these modifications have only slightly increased the accuracy of the new models in predicting future events (30,31). The PROSPECT, VIVA (VH-IVUS in Vulnerable Atherosclerosis), and PREDICTION (Prediction of Progression of Coronary Artery Disease and Clinical Outcome Using Vascular Profiling of Shear Stress and Wall Morphology) studies provided robust evidence that atheroma burden and the TCFA phenotype are strongly associated with plaque vulnerability (6,32,33). The present analysis for the first time showed that the coronary plaque phenotype, which is independently associated with nonculprit lesion–related MACE, cannot be predicted by the clinical and angiographic findings, emphasizing the potential value of more comprehensive plaque characterization (with either intravascular or noninvasive imaging) for more accurate risk stratification. Advances in intravascular imaging are expected to allow complete plaque characterization, and thus, an assessment of the whole coronary tree with upcoming invasive imaging techniques is anticipated to allow more accurate
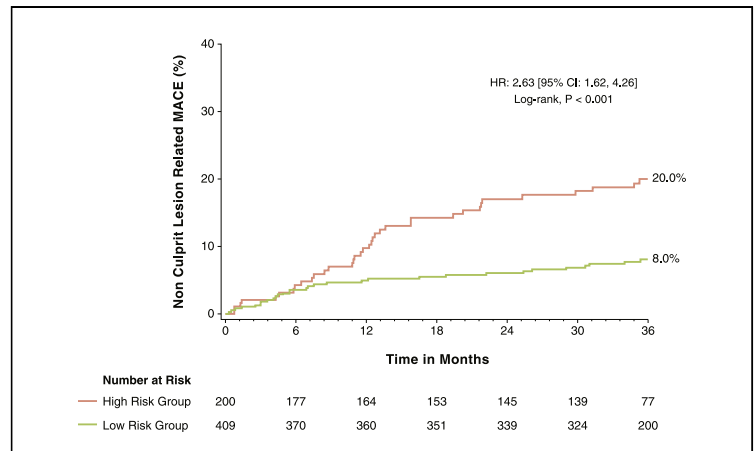

Figure 1. Prognosis in the High-Risk and Low-Risk Groups

Kaplan-Meier curves showing the nonculprit lesion-related major adverse cardiac event (MACE) rate in the high-risk (n = 200) and low-risk (n = 409) groups. CI = confidence interval; HR = hazard ratio.
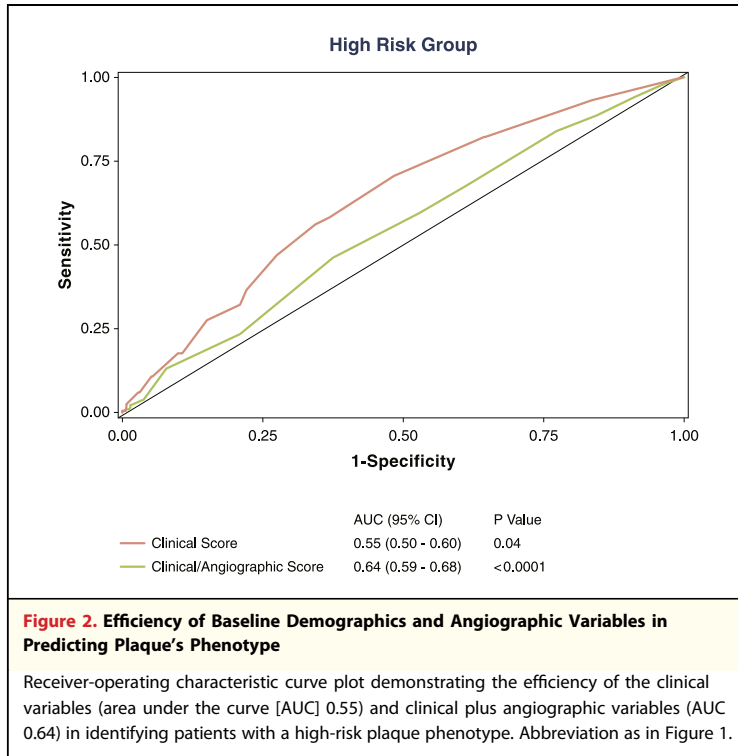
risk stratification (34). However, the additional time and cost, risk of complications, increased time required to process the obtained data, and lack of evidence about how we should treat high-risk patients make unrealistic the regular application of 3-vessel invasive imaging in clinical settings.

Noninvasive imaging carries a great potential because it overcomes the abovementioned limitations of intravascular imaging modalities. Computed tomographic coronary angiography appears able to provide information about the type of plaque, and there are robust data demonstrating its prognostic value in asymptomatic or symptomatic stable patients (34,35). Nevertheless, further research is required to

Table 4. Variables Associated With the High-Risk Group

	Odds Ratio (95% CI)	p Value
Clinical characteristics		
Increasing systolic blood pressure, per 10 mm Hg	1.07 (0.99–1.15)	0.111
History of diabetes	1.48 (0.96–2.28)	0.07
Increasing Framingham risk score, per unit	1.05 (1.00–1.11)	0.048
History of hypertension	1.31 (0.93–1.85)	0.17
Presence of metabolic syndrome	1.32 (0.93–1.86)	0.12
Angiographic characteristics		
Number of culprit vessels	1.46 (1.01–2.10)	0.042
Number of epicardial vessels with lesions	1.27 (1.06–1.51)	0.008
Number of nonculprit lesions	1.23 (1.12–1.34)	<0.0001
Number of side branches with nonculprit lesions	2.04 (1.43–2.91)	<0.0001
Total length of nonculprit lesions, per mm	1.02 (1.01–1.03)	<0.0001
CI = confidence interval.		

Figure 2. Efficiency of Baseline Demographics and Angiographic Variables in Predicting Plaque's Phenotype

Receiver-operating characteristic curve plot demonstrating the efficiency of the clinical variables (area under the curve [AUC] 0.55) and clinical plus angiographic variables (AUC 0.64) in identifying patients with a high-risk plaque phenotype. Abbreviation as in Figure 1.

examine its potential predictive ability in patients with acute myocardial infarction.

Study limitations. The criteria used to categorize patients into the high-risk and low-risk groups in the present study were based on the findings from the PROSPECT trial, in which lesions exhibiting
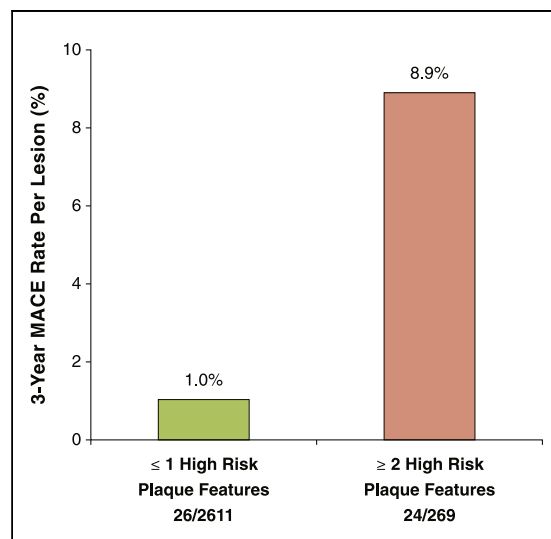

Figure 3. Event Rate at a Lesion Level

MACE rate at 3 years for lesions with no or only 1 high-risk characteristic and for those with 2 or 3 high-risk features. Abbreviation as in Figure 1.

≥2 high-risk plaque characteristics had a 9-fold incidence to progress and cause future MACE within 3 years compared with lesions having ≤1 high-risk plaque characteristics (Fig. 3). Although recently the VIVA study reported that the same IVUS-derived characteristics were associated with future adverse cardiac events (i.e., the presence of a TCFA, plaque burden ≥70%, and MLA ≤4 mm^2), the criteria of our study requires prospective validation in future studies. In addition, most of the MACE reported in the PROSPECT trial were due to repeat hospitalizations for stable or unstable angina symptoms, and thus, it is unclear whether the high-risk plaque characteristics used in this analysis to classify patients are able to predict nonculprit-related cardiac death or myocardial infarction. Fractional flow reverse evaluation was not part of the protocol in the PROSPECT study. Therefore, it is likely that hemodynamically significant lesions were left untreated during the index procedure and caused future events that may have affected the reported results.

The strict inclusion criteria used in the PROSPECT trial (e.g., patients with severe renal failure or ejection fraction <30% were excluded from the analysis) may have affected the reported association between baseline characteristics and the phenotype of the plaque. With only 609 patients in the present study, we lacked the power to identify modest relationships between all risk factors and high-risk plaque phenotype. Finally, IVUS-VH imaging has limitations, including the only moderate radial resolution and limited capability to detect the composition of the atheroma behind calcium deposits, which may have affected the results of this analysis (36,37).

CONCLUSIONS

The present study demonstrated that clinical variables have poor discrimination in detecting which patients presenting with ACS have high-risk nonculprit plaques. The addition of angiographic findings only slightly improved the accuracy of the developed model but not to the extent the need was obviated for more comprehensive plaque characterization. Future studies of invasive and noninvasive plaque evaluation may be useful in identifying patients who remain high risk after being successfully treated for ACS.

Reprint requests and correspondence: Dr. Patrick W. Serruys, ThoraxCenter, Erasmus Medical Center, 's-Gravendijkwal 230, 3015 CE Rotterdam, the Netherlands. *E-mail: p.w.j.c.serruys@erasmusmc.nl.*

REFERENCES

1. Mehta SK, McCrary JR, Frutkin AD, Dolla WJ, Marso SP. Intravascular ultrasound radiofrequency analysis of coronary atherosclerosis: an emerging technology for the assessment of vulnerable plaque. Eur Heart J 2007; 28:1283–8.

2. Garcia-Garcia HM, Mintz GS, Lerman A, et al. Tissue characterisation using intravascular radiofrequency data analysis: recommendations for acquisition, analysis, interpretation and reporting. EuroIntervention 2009;5:177–89.

3. Hong MK, Mintz GS, Lee CW, et al. A three-vessel virtual histology intravascular ultrasound analysis of frequency and distribution of thin-cap fibroatheromas in patients with acute coronary syndrome or stable angina pectoris. Am J Cardiol 2008;101:568–72.

4. Rodriguez-Granillo GA, Garcia-Garcia HM, Mc Fadden EP, et al. In vivo intravascular ultrasound-derived thin-cap fibroatheroma detection using ultrasound radiofrequency data analysis. J Am Coll Cardiol 2005; 46:2038–42.

5. Kubo T, Maehara A, Mintz GS, et al. The dynamic nature of coronary artery lesion morphology assessed by serial virtual histology intravascular ultrasound tissue characterization. J Am Coll Cardiol 2010;55:1590–7.

6. Stone GW, Maehara A, Lansky AJ, et al. A prospective natural-history study of coronary atherosclerosis. N Engl J Med 2011;364:226–35.

7. Serruys PW, Garcia-Garcia HM, Buszman P, et al. Effects of the direct lipoprotein-associated phospholipase A$_2$ inhibitor darapladib on human coronary atherosclerotic plaque. Circulation 2008;118:1172–82.

8. Falk E. Plaque rupture with severe pre-existing stenosis precipitating coronary thrombosis. Characteristics of coronary atherosclerotic plaques underlying fatal occlusive thrombi. Br Heart J 1983;50:127–34.

9. Marso SP, Mercado N, Maehara A, et al. Plaque composition and clinical outcomes in acute coronary syndrome patients with metabolic syndrome or diabetes. J Am Coll Cardiol Img 2012; 5:S42–52.

10. Philipp S, Bose D, Wijns W, et al. Do systemic risk factors impact invasive findings from virtual histology? Insights from the International Virtual Histology Registry. Eur Heart J 2010; 31:196–202.

11. Marso SP, Frutkin AD, Mehta SK, et al. Intravascular ultrasound measures of coronary atherosclerosis are associated with the Framingham risk score: an analysis from a global IVUS registry. EuroIntervention 2009;5:212–8.

12. Baber U, Stone GW, Weisz G, et al. Coronary plaque composition, morphology, and outcomes in patients with and without chronic kidney disease presenting with acute coronary syndromes. J Am Coll Cardiol Img 2012;5:S53–61.

13. Missel E, Mintz GS, Carlier SG, et al. In vivo virtual histology intravascular ultrasound correlates of risk factors for sudden coronary death in men: results from the prospective, multi-centre virtual histology intravascular ultrasound registry. Eur Heart J 2008;29:2141–7.

14. Arroyo-Espliguero R, Avanzas P, Cosin-Sales J, Aldama G, Pizzi C, Kaski JC. C-reactive protein elevation and disease activity in patients with coronary artery disease. Eur Heart J 2004;25:401–8.

15. Orn S, Manhenke C, Ueland T, et al. C-reactive protein, infarct size, microvascular obstruction, and left-ventricular remodelling following acute myocardial infarction. Eur Heart J 2009;30:1180–6.

16. de Beer FC, Hind CR, Fox KM, Allan RM, Maseri A, Pepys MB. Measurement of serum C-reactive protein concentration in myocardial ischaemia and infarction. Br Heart J 1982;47:239–43.

17. Brennan ML, Reddy A, Tang WH, et al. Comprehensive peroxidase-based hematologic profiling for the prediction of 1-year myocardial infarction and death. Circulation 2010;122:70–9.

18. Elesber AA, Conover CA, Denktas AE, et al. Prognostic value of circulating pregnancy-associated plasma protein levels in patients with chronic stable angina. Eur Heart J 2006;27:1678–84.

19. Thompson A, Gao P, Orfei L, et al. Lipoprotein-associated phospholipase A$_2$ and risk of coronary disease, stroke, and mortality: collaborative analysis of 32 prospective studies. Lancet 2010; 375:1536–44.

20. Tada S, Tarbell JM. A computational study of flow in a compliant carotid bifurcation-stress phase angle correlation with shear stress. Ann Biomed Eng 2005;33:1202–12.

21. Prins BP, Lagou V, Asselbergs FW, Snieder H, Fu J. Genetics of coronary artery disease: genome-wide association studies and beyond. Atherosclerosis 2012;225:1–10.

22. Lee SW, Antiga L, Spence JD, Steinman DA. Geometry of the carotid bifurcation predicts its exposure to disturbed flow. Stroke 2008; 39:2341–7.

23. Zynda TK, Thompson CD, Hoang KC, et al. Disparity between angiographic coronary lesion complexity and lipid core plaques assessed by near-infrared spectroscopy. Catheter Cardiovasc Interv 2013;81:529–37.

24. Halkin A, Singh M, Nikolsky E, et al. Prediction of mortality after primary percutaneous coronary intervention for acute myocardial infarction: the CADILLAC risk score. J Am Coll Cardiol 2005;45:1397–405.

25. Eagle KA, Lim MJ, Dabbous OH, et al. A validated prediction model for all forms of acute coronary syndrome: estimating the risk of 6-month post-discharge death in an international registry. JAMA 2004;291:2727–33.

26. Addala S, Grines CL, Dixon SR, et al. Predicting mortality in patients with ST-elevation myocardial infarction treated with primary percutaneous coronary intervention (PAMI risk score). Am J Cardiol 2004;93:629–32.

27. Morrow DA, Antman EM, Charlesworth A, et al. TIMI risk score for ST-elevation myocardial infarction: a convenient, bedside, clinical score for risk assessment at presentation: an intravenous nPA for treatment of infarcting myocardium early II trial substudy. Circulation 2000;102:2031–7.

28. Palmerini T, Caixeta A, Genereux P, et al. Comparison of clinical and angiographic prognostic risk scores in patients with acute coronary syndromes: analysis from the Acute Catheterization and Urgent Intervention Triage StrategY (ACUITY) trial. Am Heart J 2012;163:383–91.

29. Lev EI, Kornowski R, Vaknin-Assa H, et al. Comparison of the predictive value of four different risk scores for outcomes of patients with ST-elevation acute myocardial infarction undergoing primary percutaneous coronary intervention. Am J Cardiol 2008;102:6–11.

30. Garg S, Sarno G, Serruys PW, et al. Prediction of 1-year clinical outcomes using the SYNTAX score in patients with acute ST-segment elevation myocardial infarction undergoing primary percutaneous coronary intervention: a substudy of the STRATEGY (Single High-Dose Bolus Tirofiban and Sirolimus-Eluting Stent Versus Abciximab and Bare-Metal Stent in Acute Myocardial Infarction) and MULTISTRATEGY (Multicenter Evaluation of Single High-Dose Bolus Tirofiban Versus Abciximab With Sirolimus-Eluting Stent or Bare-Metal Stent in Acute Myocardial Infarction Study) trials. J Am Coll Cardiol Intv 2011;4:66–75.

31. Damman P, Beijk MA, Kuijt WJ, et al. Multiple biomarkers at admission significantly improve the prediction of mortality in patients undergoing primary percutaneous coronary intervention for acute ST-segment elevation myocardial infarction. J Am Coll Cardiol 2011;57:29–36.

32. Stone PH, Saito S, Takahashi S, et al. Prediction of progression of coronary artery disease and clinical outcomes using vascular profiling of endothelial shear stress and arterial plaque characteristics: the PREDICTION study. Circulation 2012;126:172–81.

33. Calvert PA, Obaid DR, O'Sullivan M, et al. Association between IVUS findings and adverse outcomes in patients with coronary artery disease: the VIVA (VH-IVUS in Vulnerable Atherosclerosis) study. J Am Coll Cardiol Img 2011;4:894–901.

34. Motoyama S, Sarai M, Harigaya H, et al. Computed tomographic angiography characteristics of atherosclerotic plaques subsequently resulting in acute coronary syndrome. J Am Coll Cardiol 2009;54:49–57.

35. Villines TC, Hulten EA, Shaw LJ, et al. Prevalence and severity of coronary artery disease and adverse events among symptomatic patients with coronary artery calcification scores of zero undergoing coronary computed tomography angiography: results from the CONFIRM (Coronary CT Angiography Evaluation for Clinical Outcomes: an International Multicenter) registry. J Am Coll Cardiol 2011;58:2533–40.

36. Sales FJ, Falcão BA, Falcão JL, et al. Evaluation of plaque composition by intravascular ultrasound "virtual histology": the impact of dense calcium on the measurement of necrotic tissue. EuroIntervention 2010;6:394–9.

37. Thim T, Hagensen MK, Wallace-Bradley D, et al. Unreliable assessment of necrotic core by virtual histology intravascular ultrasound in porcine coronary artery disease. Circ Cardiovasc Imaging 2010;3:384–91.

38. Levey AS, Bosch JP, Lewis JB, Greene T, Rogers N, Roth D. A more accurate method to estimate glomerular filtration rate from serum creatinine: a new prediction equation. Modification of Diet in Renal Disease Study Group. Ann Intern Med 1999; 130:461–70.

Key Words: cardiovascular events ■ coronary angiography ■ intravascular ultrasound.

▶ **APPENDIX**

For a supplemental table, please see the online version of this article.